Supporting Information

Hydrogen Spillover at sub 2 nm Pt Nanoparticles by Electrochemical Hydrogen Loading

Somik Mukherjee[1], Balavinayagam Ramalingam[1], and Shubhra Gangopadhyay[1,2,*]

1. Department of Electrical Engineering, University of Missouri – Columbia
2. Nanos Technologies LLC, Columbia, MO

Fabrication of Pt sputtered HOPG-FTO substrates – The base FLG-FTO (few layer graphene – fluorine doped tin oxide) substrate was prepared by rubbing highly ordered pyrolytic graphite (HOPG – SPI2) block on rough FTO coated glass substrates for 3 min each. Scotch tape removal of the loosely bound graphitic flakes was done 3 times for each sample to leave behind a relatively uniform graphite-FTO composite on the substrates. All substrates were rinsed using AMD wash (acetone, methanol and DI water) to remove any organic residue from the scotch tape. After the rinsing step, Pt was sputtered using the TTS configuration at 30 W for varying deposition times (10 s, 20 s, 30 s, 45 s, 60 s and 120 s). More details of the sputtering process can be found in our previous works [1, 2].

RAMAN characterization of FLG substrates – RAMAN spectroscopy using a 514 nm laser was done at 3 marked spots on each Pt sputtered FTO-FLG sample (total 18 samples) to determine the quality of the FLG film and the uniformity of the I_D/I_G ratio at different spots across varying samples. The RAMAN was done at standard confocality because, given the high surface roughness of FTO, weak signals were attained at high confocality. The RAMAN curves and the mean and standard deviations of the I_D/I_G ratios are listed below.

The typical image profile of Pt sputtered-HOPG-FTO substrates as seen through a 50X objective microscope under white light is displayed below in Figure S1. The obtained normalized RAMAN curves for each Pt varying sputtered-HOPG-FTO sample are listed below in Figure S2. It can be seen that even after prolonged sputtering time, there is minimal plasma damage to the FLG film surface as the I_D/I_G ratio remains consistent.

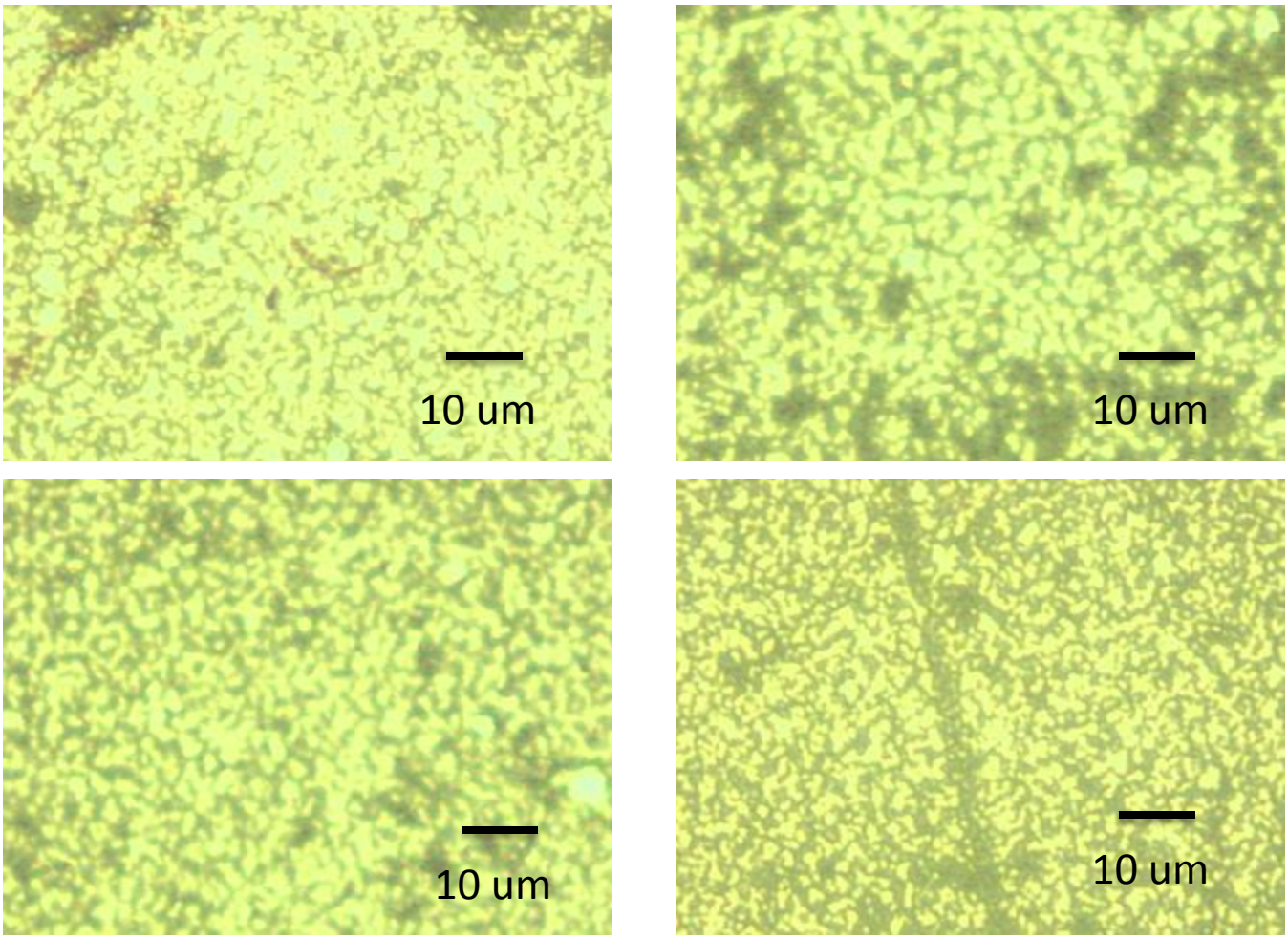

Figure S1: Image profiles for typical Pt sputtered-HOPG-FTO substrates as viewed through a 50X objective on the RAMAN microscope

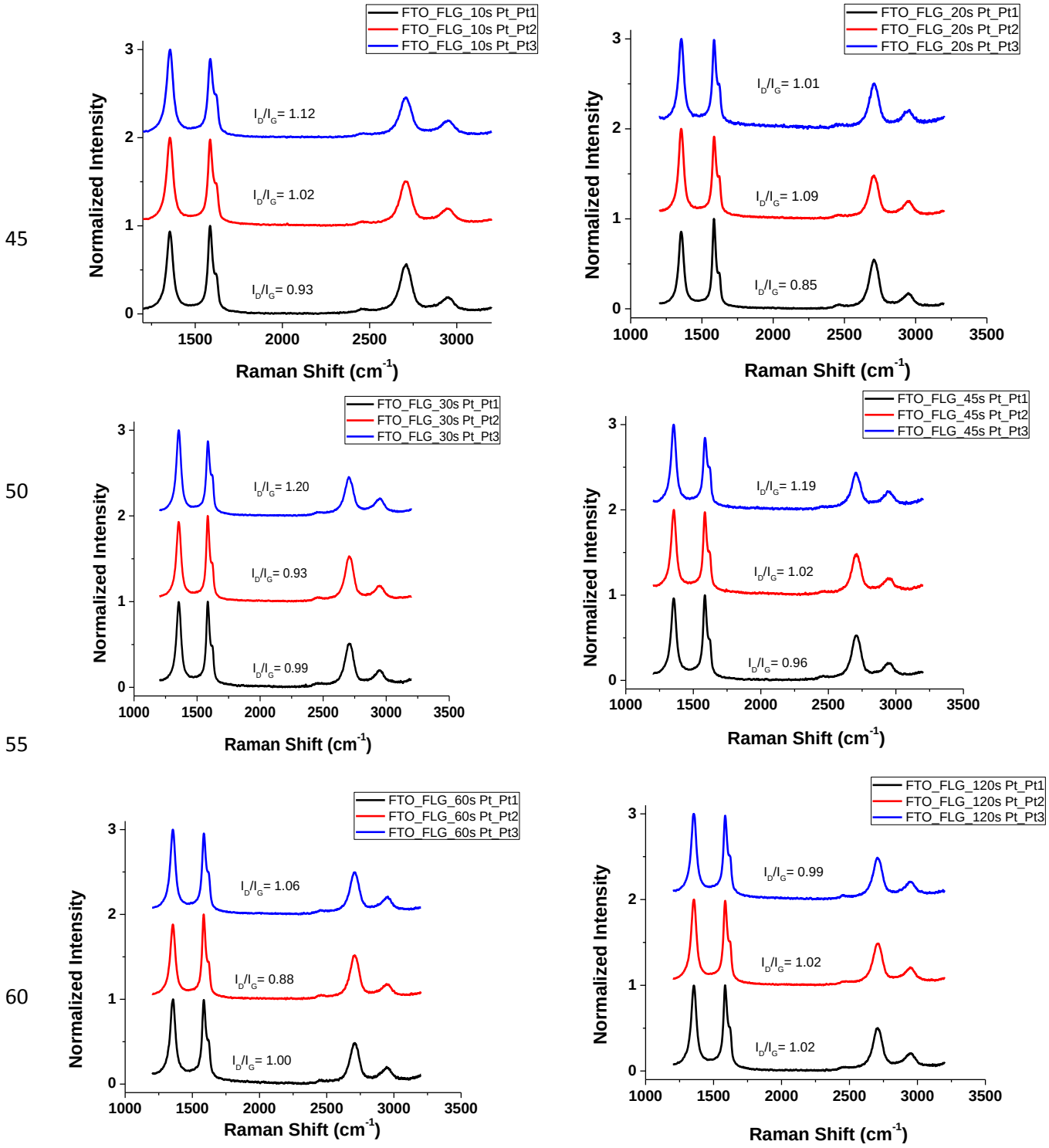

Figure S2: Normalized RAMAN curves at 3 marked spots for Pt varying sputtered-HOPG-FTO sample - (a) 10 s Pt, (b) 20 s Pt, (c) 30 s Pt, (d) 45 s Pt, (e) 60 s Pt, (f) 120 s Pt

For all the RAMAN curves, the I_D/I_G ratio seems quite similar. The 2D band for all the samples is around 2705 cm^{-1} which is characteristic of approx. 3-4 graphene layers [3]. The slight peak noticeable around 2940 cm^{-1} in each sample is generally attributed to a two-phonon excitation. The energy corresponds to the sum of the 1355 and 1590 cm^{-1}. This indicates that these two modes occur in the same region of the sample [4, 5]. Table S1 lists the average Pt nanoparticle diameter, I_D/I_G ratio for each sample at 3 different spots with the mean and standard deviation for each sample. The overall mean of the I_D/I_G ratio for all 18 samples was 1.02 and the standard deviation was 0.09 revealing a < 10% error bar.

Pt deposition time on HOPG-FTO substrate (s)	Avg. Nanoparticle Size	I_D/I_G Spot 1	I_D/I_G Spot 2	I_D/I_G Spot 3	I_D/I_G mean	I_D/I_G Std. Dev
10	<0.7 nm	0.93	1.02	1.12	1.02	0.09
20	0.9 nm	0.85	1.09	1.01	0.98	0.12
30	1.2 nm	0.99	0.93	1.20	1.04	0.14
45	1.5 nm	0.96	1.02	1.19	1.06	0.11
60	Nano-islands	1	0.88	1.06	0.98	0.09
120	Nano-islands	1.02	1.02	0.99	1.01	0.02

Table S1: I_D/I_G ratio for each sample at 3 different marked spots with the mean and standard deviation for each sample

Based on the RAMAN data, the FLG-FTO composite films look uniform enough to analyze the hydrogen storage properties when used in spillover experiments. Theoretically, if hydrogen is stored on the carbon, the D band should go up and the G band should go down due to the formation of more sp^3 bonds. Availability of more defect sites might help enhance the hydrogen storage capability of the fabricated HOPG-FTO composite films.

XPS characterization of Pt-FLG substrates after H loading – X-ray photoelectron spectroscopy (XPS) was conducted using a Kratos Axis 165 spectrometer and vacuum level within the chamber remained near 1.0×10^{-8} Torr during acquisition. A 150 W Al X-ray source was used for the XPS measurements and any effects of sample charging were accounted for by fixing the oxygen peak. The different time sputtered Pt - FLG samples were cycled in the H_{UPD} region for 250 cycles each and XPS analysis was performed on the substrate surface before and after potentiometric cycling to study the possibility of change in sp^2 C-C to sp^3 C-H bonds on the FLG surface. In figure S3, the tail broadening in higher binding energy region of the c-1s region in the XPS spectra is indicative of C-O contamination and peaks indicative of these contaminants can be fitted around 286.1 (C-OH), 287.5 (C=O) and 288.9 eV (O=C-OH) and the resultant fit yields an r^2 values around 0.998. These peak positions within the C-1s region were obtained from XPS analysis of graphene and reduced graphene oxide samples reported before in published literature[6-15]. For the analysis of the XPS spectra in terms of contributions from individual components representing different species, the experimental spectra were fitted by a combination of components by minimizing the total squared-error of the fit. Individual components were represented by a convolution of Lorenztian function, representing the life-time broadening, and a Gaussian function to account for the instrumental

resolution [16]. The Gaussian broadening was kept the same for different components. A Shirley background function was also considered to account for the inelastic background in the XPS spectra. In the C-1s region, the C-C peak position was fixed at 284.7 (± 0.1 eV) and the FWHM was fitted within a (± 0.05 eV range).

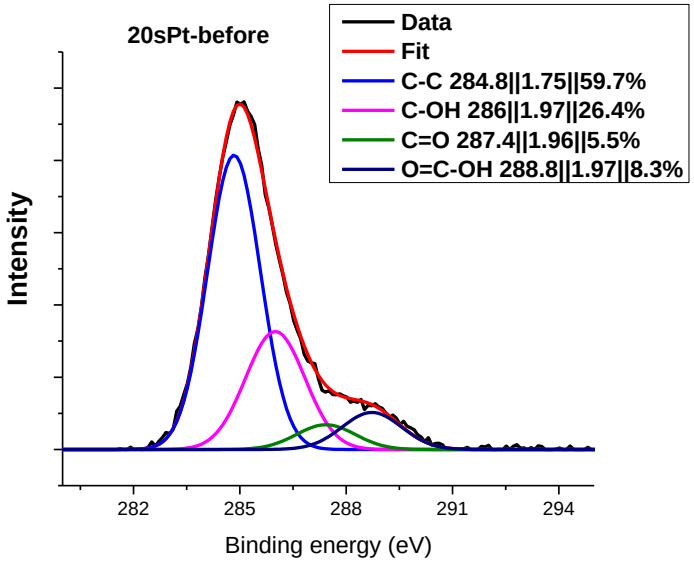

Figure S3: Deconvoluted XPS spectra of 20s Pt decorated FLG substrate before electrochemical H loading. The peak position || FWHM || percentage area contribution of the peak towards the overall fit, are displayed in the curve

Figure S4 shows the XPS spectra of Pt-FLG sample before and after electrochemical H loading. The FWHM of the XPS spectra are also reported within the plot. It can be see that after H loading, only in the case of 20s Pt (0.9 nm mean diameter) -FLG sample, significant change in FWHM can be seen. The FWHM increases from 2.16 to 2.49 after H loading which corresponds to additional carbon bonding in the C-1s region.

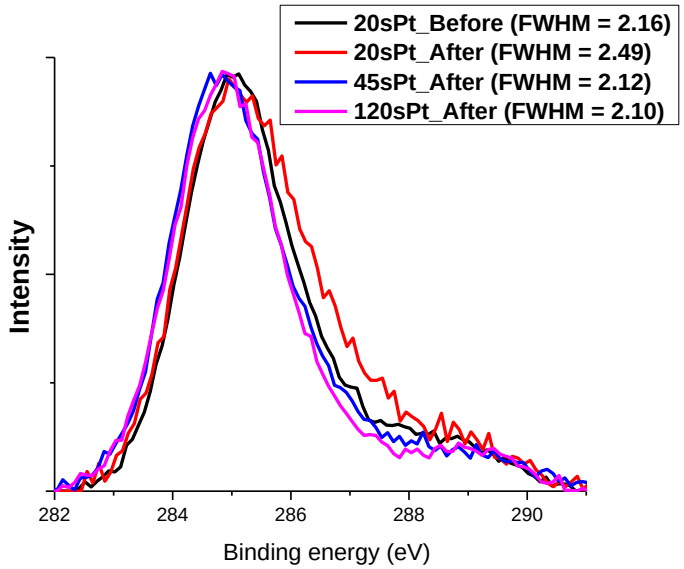

Figure S4: XPS spectra of various Pt (different sputtering times 20s, 45s, 120s) decorated FLG substrate before and after electrochemical H loading. The FWHM of the overall C-1s region is also reported in the curve

Figure S5 displays the XPS spectra of 20s Pt- FLG with its deconvoluted peaks. Keeping the rest of the components (C-C, C-OH, C=O and O=C-OH) at constant peak positions and by limiting the lineshape of the C-C peak, the best fitting was obtained by adding an additional peak at 285.3 eV. This peak can be attributed to the binding energy of the C-H bond. The peak position of the C-H bond has been reported to be ~0.65 eV greater than the C-C bond [11]. Only in the 20 s Pt decorated FLG sample, the need to incorporate an additional peak at 285.3 eV was realized. This can be interpreted as successful partial hydrogenation of the C-C bonds in the FLG substrate.

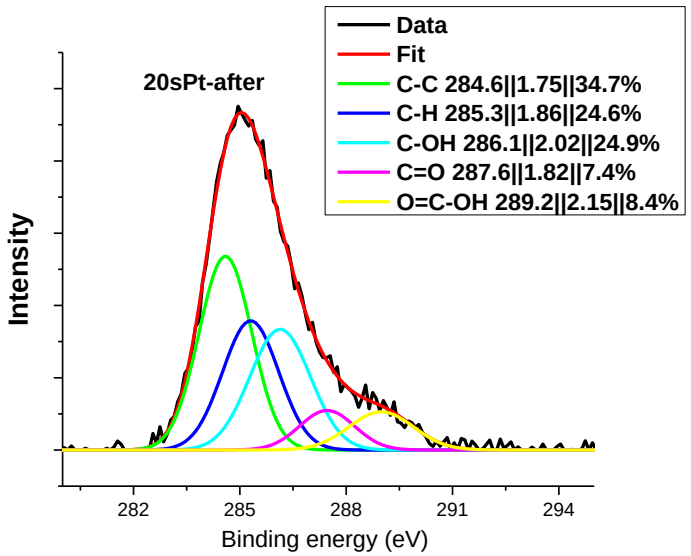

Figure S5: Deconvoluted XPS spectra of 20s Pt decorated FLG substrate after electrochemical H loading. The peak position || FWHM || percentage area contribution of the peak towards the overall fit, are reported in the curve

Figures 4 and 5 display the XPS spectra of 45 s Pt (mean size = 1.5 nm) and 120 s Pt (formation of nano islands) decorated FLG substrates after H loading. During deconvolution, incorporation of an additional peak at 285.3 eV was not required to fit the XPS data. Thus, based on previously performed electrochemical characterization and XPS analysis, it can be concluded that only in case of 0.9 nm Pt (20 s) nanoparticles, there is a high enough degree of spillover and the spilled over H atoms have enough energy to overcome the activation energy barrier to form C-H bonds.

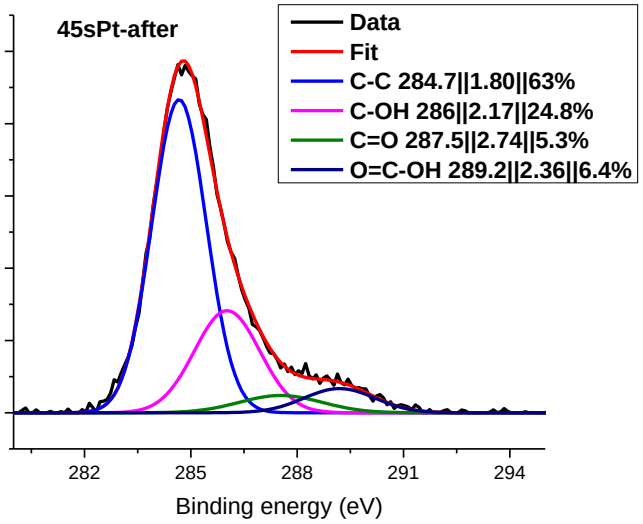

Figure S6: Deconvoluted XPS spectra of 45 s Pt decorated FLG substrate after electrochemical H loading. The peak position || FWHM || percentage area contribution of the peak towards the overall fit, are reported in the curve

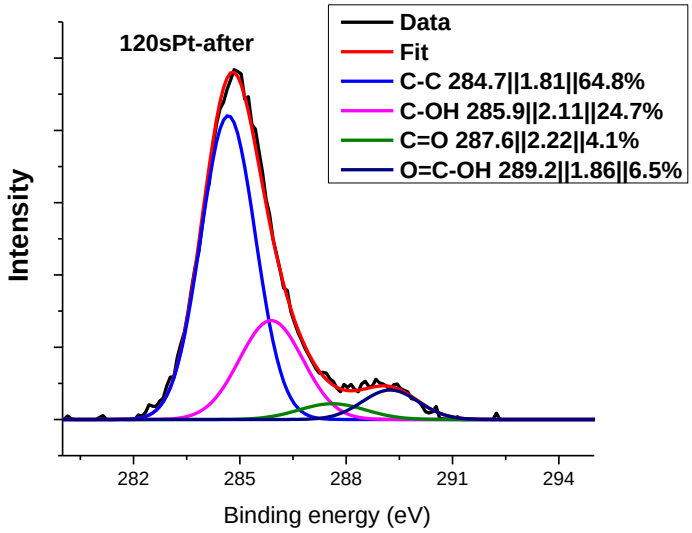

Figure S7: Deconvoluted XPS spectra of 120 s Pt decorated FLG substrate after electrochemical H loading. The peak position || FWHM || percentage area contribution of the peak towards the overall fit, are reported in the curve

All the XPS peak fitting parameters, i.e., peak position, FWHM and percentage composition to overall fit are presented below in table S2. It must be noted that there is a slight C-C peak broadening upon incorporation of bigger Pt nanoparticles (45s Pt and 120s Pt). C-C peak broadening due to Incorporation of metal nanoparticles has been observed before in [17]. This has been attributed to the influence of metal-carbon interaction which disrupts the C-C binding energy and broadens the lineshape of the C-C peak.

Sample	C-C	C-H	C-OH	C=O	O=C-OH

20sPt_Before (FWHM = 2.16 eV)	284.8‖1.75‖59.7%	-	286‖1.97‖26.4%	287.4‖1.96‖5.5%	288.8‖1.97‖8.3%
20sPt_After (FWHM = 2.49 eV)	284.6‖1.75‖34.7%	285.3‖1.86 ‖24.6%	286.1‖2.02‖24.9%	287.5‖1.82‖7.4%	289.0‖2.15‖8.4%
45sPt_After (FWHM = 2.12 eV)	284.7‖1.80‖63%	-	286‖2.17‖24.8%	287.5‖2.74‖5.3%	289.2‖2.36‖6.4%
120sPt_After (FWHM = 2.10 eV)	284.7‖1.81‖64.8%	-	285.9‖2.11‖24.7%	287.6‖2.22‖4.1%	289.2‖1.86‖6.5%

Table S2: XPS fitting parameters of various peaks used to for the XPS spectra

References

1. R. Balavinayagam, M. Somik, J. M. Cherian, G. Keshab and G. Shubhra, *Nanotechnology*, 2013, 24, 205602.
2. M. Somik, R. Balavinayagam, G. Lauren, H. Steven, A. B. Gary, F. Phil, S. Shramik and G. Shubhra, *Nanotechnology*, 2012, 23, 485405.
3. Z. Ni, Y. Wang, T. Yu and Z. Shen, *Nano Research*, 2008, 1, 273-291.
4. R. J. Nemanich, J. T. Glass, G. Lucovsky and R. E. Shroder, *Raman scattering characterization of carbon bonding in diamond and diamondlike thin films*, AVS, 1988.
5. R. E. Shroder, R. J. Nemanich and J. T. Glass, *Physical Review B*, 1990, 41, 3738.
6. Z. Luo, J. Shang, S. Lim, D. Li, Q. Xiong, Z. Shen, J. Lin and T. Yu, *Applied Physics Letters*, 2010, 97, 233111.
7. A. V. Murugan, T. Muraliganth and A. Manthiram, *Chemistry of Materials*, 2009, 21, 5004-5006.
8. X. Li, G. Zhang, X. Bai, X. Sun, X. Wang, E. Wang and H. Dai, *Nat Nano*, 2008, 3, 538-542.
9. L. Tang, Y. Wang, Y. Li, H. Feng, J. Lu and J. Li, *Advanced Functional Materials*, 2009, 19, 2782-2789.
10. D. Yang, A. Velamakanni, G. Bozoklu, S. Park, M. Stoller, R. D. Piner, S. Stankovich, I. Jung, D. A. Field, C. A. Ventrice Jr and R. S. Ruoff, *Carbon*, 2009, 47, 145-152.
11. A. Nikitin, L.-Å. Näslund, Z. Zhang and A. Nilsson, *Surface Science*, 2008, 602, 2575-2580.

12. A. Pirkle, J. Chan, A. Venugopal, D. Hinojos, C. W. Magnuson, S. McDonnell, L. Colombo, E. M. Vogel, R. S. Ruoff and R. M. Wallace, *Applied Physics Letters*, 2011, 99, 122108.
13. J. Campos-Delgado, J. M. Romo-Herrera, X. Jia, D. A. Cullen, H. Muramatsu, Y. A. Kim, T. Hayashi, Z. Ren, D. J. Smith, Y. Okuno, T. Ohba, H. Kanoh, K. Kaneko, M. Endo, H. Terrones, M. S. Dresselhaus and M. Terrones, *Nano Letters*, 2008, 8, 2773-2778.
14. Z. Luo, T. Yu, K.-j. Kim, Z. Ni, Y. You, S. Lim, Z. Shen, S. Wang and J. Lin, *ACS nano*, 2009, 3, 1781-1788.
15. S. Bae, H. Kim, Y. Lee, X. Xu, J.-S. Park, Y. Zheng, J. Balakrishnan, T. Lei, H. Ri Kim, Y. I. Song, Y.-J. Kim, K. S. Kim, B. Ozyilmaz, J.-H. Ahn, B. H. Hong and S. Iijima, *Nat Nano*, 2010, 5, 574-578.
16. D. Choudhury, B. Das, D. D. Sarma and C. N. R. Rao, *Chemical Physics Letters*, 2010, 497, 66-69.
17. A. Y. Vasil'kov, A. V. Naumkin, I. O. Volkov, V. L. Podshibikhin, G. V. Lisichkin and A. R. Khokhlov, *Surface and Interface Analysis*, 2010, 42, 559-563.